Volume 6 | Number 44 | 28 November 2018 | Pages 11759–12106

Journal of Materials Chemistry C

Materials for optical, magnetic and electronic devices

rsc.li/materials-c

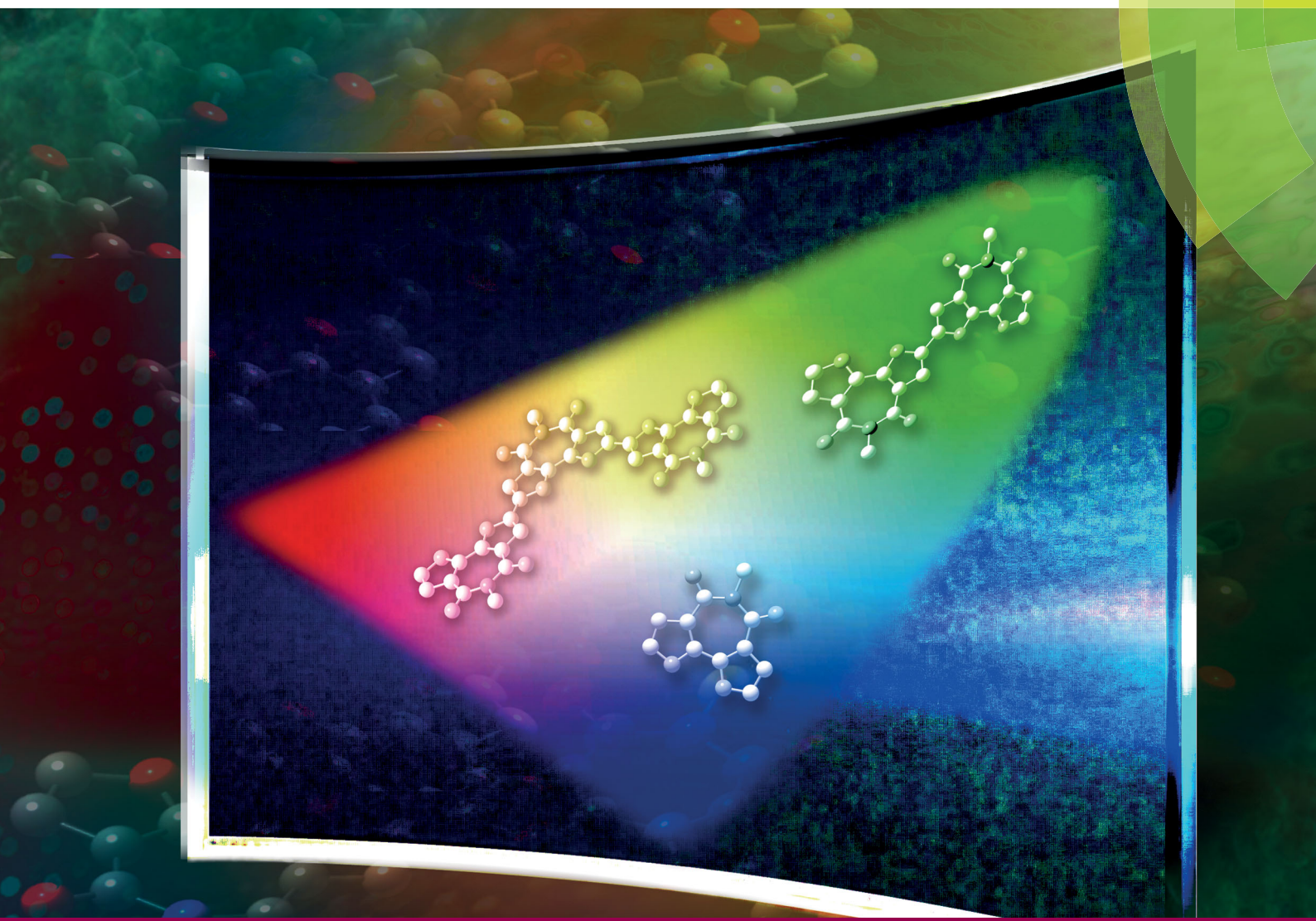

Themed issue: Emerging Investigators 2018

ISSN 2050-7526

ROYAL SOCIETY OF CHEMISTRY

COMMUNICATION

Ori Gidron *et al.*

Bifuran-imide: a stable furan building unit for organic electronics

Journal of Materials Chemistry C

COMMUNICATION

Check for updates

Cite this: J. Mater. Chem. C, 2018, 6, 11951

Received 13th June 2018, Accepted 9th August 2018

DOI: 10.1039/c8tc02908c

rsc.li/materials-c

Bifuran-imide: a stable furan building unit for organic electronics†

Sandip V. Mulay,[a] Benny Bogoslavky,[b] Idan Galanti,[a] Ehud Galun[c] and Ori Gidron *[a]

Oligo- and polyfurans hold many advantages over their thiophene analogues, yet their low environmental stability greatly limits their applications. In this work, we introduce a new building unit, bifuran-imide (BFI), which displays many of the advantageous properties observed for oligofurans, such as strong fluorescence, high solubility, significant quinoid character, and planarity, while also being significantly more stable (both thermally and photochemically) than parent oligofurans. Oligomers and polymers containing BFI show good solid state packing, strong fluorescence, and solubility, which makes them ideal candidates for active materials in organic electronics.

The field of organic electronics depends on the discovery of new materials whose π-conjugated backbones endow them with desired properties.[1–4] Good candidate materials are those that demonstrate small HOMO–LUMO gaps, strong fluorescence, good solid-state packing, and a planar backbone resulting in good charge delocalization and mobility. These criteria are met by only a limited number of π-conjugated backbones, with oligo- and polythiophenes (**nT**, Chart 1) and their derivatives currently dominating the field.[5–10]

We have previously introduced a new family of organic electronic materials, oligofurans (**nF**, Chart 1), which are the oxygen-containing analogues of oligothiophenes.[11–16] Oligofurans display significant advantages over oligothiophenes, such as high rigidity/planarity, strong fluorescence, extensive conjugation, good field-effect mobility, and high solubility.[17–23] These properties make oligofurans attractive candidates for devices such as organic light emitting diodes (OLEDs),[24–26] organic light emitting transistors (OLETs), and organic field-effect transistors (OFETs).[27–30]

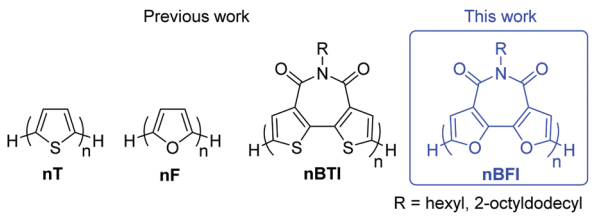

Chart 1 Structures of **nT**, **nF**, **nBTI** and **nBFI** discussed in this work.

Unlike **nT**, which are inert toward Diels–Alder cycloaddition, **nF** can serve as synthons for long oligoarenes.[31] However, oligofurans can undergo photooxidation under ambient conditions.[11] Their low environmental stability must be overcome if oligo- and polyfurans are to become useful as active materials in organic electronic devices.

Recently, bithiophene-imide (**BTI**, Chart 1) was introduced by the Marks group as an n-type semiconductor.[32,33] This building unit was successfully applied in OFETs and organic solar cells.[34,35] Ladder oligomers and polymers of **BTI** units were shown to have electron mobilities of up to 3.71 $cm^2 V^{-1} s^{-1}$ and high environmental stabilities.[36,37] Rupar's group recently reported bridged bifuran complexes stabilized by p-block elements that have a lower LUMO level through σ*–π* conjugation.[38] Considering these factors, we sought to stabilize furans by introducing the bifuran-imide (**BFI**, Chart 1) building unit.

Here, we report the synthesis of the **BFI** unit, and its corresponding oligomers and polymers (**nBFI**) bearing hexyl (**nBFI-H**) or 2-octyldodecyl (**nBFI-OD**) substituents (Chart 1). We find that **nBFI** are significantly more stable (both thermally and photochemically) compared with α-oligofurans while displaying good solid-state packing, strong fluorescence, and good solubility, which is important for their processability. These properties allowed us to obtain the high molecular weight polymer, poly(**BFI-OD**), which was also found to be soluble in a wide range of organic solvents.

The synthesis of the **BFI** monomer, dimer, trimer, and polymer is depicted in Scheme 1. In the first step, dibromobifuran (**1**)[15]

[a] Institute of Chemistry, The Hebrew University of Jerusalem, Edmond J. Safra Campus, Jerusalem, Israel. E-mail: ori.gidron@mail.huji.ac.il
[b] The Laboratory for Molecular Structure Analysis, The Institute of Chemistry, The Hebrew University of Jerusalem, The Edmond J. Safra Campus, Jerusalem, Israel
[c] Head of Materials Division, R&T Base Unit, DDR&D IMOD, Hakirya, Tel Aviv, Israel

† Electronic supplementary information (ESI) available: Experimental procedures, computational and electrochemistry details, NMR spectra, CIF files and additional data. CCDC 1839512–1839517. For ESI and crystallographic data in CIF or other electronic format see DOI: 10.1039/c8tc02908c

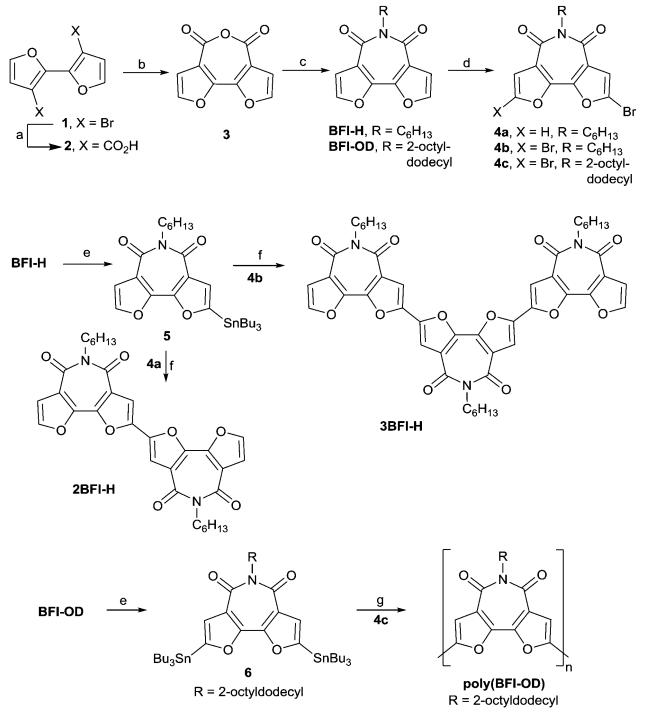

Scheme 1 Synthetic procedure for bifuran-imide building units, dimer, trimer, and homopolymer. Reagents and conditions: (a) *n*-butyllithium, dry ice, −70 °C, 7 h; (b) acetic anhydride, reflux, 12 h; (c) (i) RNH_2 (R = *n*-hexyl or 2-octyldodecyl), CH_2Cl_2, 40 °C, 12 h, (ii) $SOCl_2$, 40 °C, 15 h; (d) Br_2, $FeCl_3$ (cat.), CH_2Cl_2, room temperature; (e) lithium diisopropylamide, tributyltin chloride, tetrahydrofuran, −85 °C, 3 h; (f) $Pd(PPh_3)_4$ (*i.e.*, $Pd[(C_6H_5)_3P]_4$), toluene, 90 °C; (g) $Pd(PPh_3)_4$, dimethylformamide, 90 °C.

was converted to bifuran-dicarboxylic acid (**2**) by lithiation with *n*-butyllithium followed by addition of dry ice. Next, bifuran-dicarboxylic anhydride (**3**) was obtained in 81% yield from **2** by condensation/cyclization in refluxing acetic anhydride. The key building units, bifuran-imides **BFI-H** (88%) and **BFI-OD** (79%), were synthesized from anhydride **3** by reaction with hexylamine or 2-octyldodecylamine, respectively, followed by *in situ* treatment with $SOCl_2$.

To synthesize **2BFI-H** and **3BFI-H**, **BFI-H** was brominated with Br_2 and $FeCl_3$ to yield the monobromobifuran-imide **4a** (56%), and stannylated by lithiation with lithium diisopropylamide (LDA) followed by treatment with tributyltin chloride to give **5** (52%). The dibromobifuran-imide **4b** (97%) and **4c** (96%) were obtained using an excess of Br_2. The Stille coupling of **5** with monobromobifuran-imide (**4a**) and dibromobifuran-imide (**4b**) delivered the dimer **2BFI-H** (61%) and trimer **3BFI-H** (45%), respectively.

Attempts to synthesize the homopolymer of **BFI-H** by Stille polymerization of **4b** resulted in an insoluble polymer. In contrast, when the distannyl **BFI-OD** (**6**) was coupled with the corresponding dibromide **4c**, the resulting polymer, poly(**BFI-OD**), was found to be considerably more soluble than the hexyl analogue. This was first evident from the NMR spectrum of poly(**BFI-OD**), which could be recorded in $CDCl_3$ with no heating. For comparison, the NMR spectrum of the corresponding thiophene-based homopolymer, poly(**BTI-OD**) was recorded at 120 °C in 1,2-tetrachloroethane.[33] Gel permeation chromatography (GPC) was used to determine the polymer molecular weight *versus* polystyrene. Poly(**BFI-OD**) was found to have a molecular weight (M_w) of 27 000 Da and a polydispersity index (PDI) of 2.1, corresponding to a mean chain length of ∼60 monomer units (∼120 furan rings). This is significantly longer than for the previously reported thiophene analogue poly(**BTI-OD**), which consists of only ∼15 monomer units.[32] This difference in mean chain length reflects the better solubility of poly(**BFI-OD**), as greater solubility permits the formation of longer polymer chains. Thermogravimetric analysis (TGA) showed poly(**BFI-OD**) to have good thermal stability with less than 5% weight loss up to 350 °C (Fig. S4, ESI†). Glass phase transitions were not observed by differential calorimetry measurements for either **nBFI-H** or poly(**BFI-OD**) (Fig. S1–S4, ESI†).

The single X-ray crystal structures of **3**, **BFI-H**, and **2BFI-H** were obtained by slow diffusion of hexane into dichloromethane at room temperature. Both the anhydride **3** and imide **BFI-H** (Fig. 1a and b) display planar conformations with the C–C bond length between two furan rings measured at 1.425 Å and 1.418 Å, respectively. These distances are slightly shorter than the C–C bond length (1.430 Å) previously reported phosphorus bridged bifurans.[38] The dimer **2BFI-H** displays even shorter C–C bond lengths between the two furans in the same imide unit (1.403 Å and 1.407 Å) and an interunit bond length of 1.425 Å (Fig. 1c). Additionally, no torsion is observed between the two **BFI** units, which is an indication of the strong quinoid character of this π-conjugated backbone. One factor which contributes to the stronger quinoid character of **2BFI-H** is the lower aromaticity of furan compared with its thiophene analogues.[22] In addition, the larger *exo* angles in furan often associated with the planar its backbone, and consequently with increased conjugation.[16] **BFI-H** and **2BFI-H** show π–π interactions in a parallel-displaced manner with interplanar distances of 3.31–3.51 Å and 3.20–3.36 Å, respectively (Fig. 2).

The absorption and emission spectra of **nBFI-H**, **BFI-OD**, and poly(**BFI-OD**) in chloroform are displayed in Fig. 3a and b with

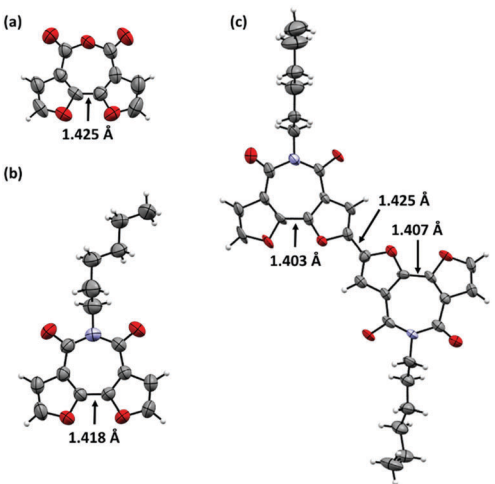

Fig. 1 ORTEP representation of (a) **3**; (b) **BFI-H**; and (c) **2BFI-H**.

This journal is © The Royal Society of Chemistry 2018

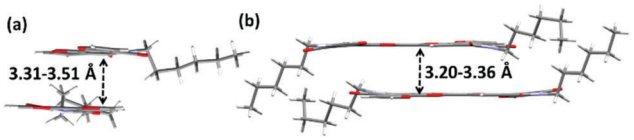

Fig. 2 Solid state packing of (a) **BFI-H**; and (b) **2BFI-H**.

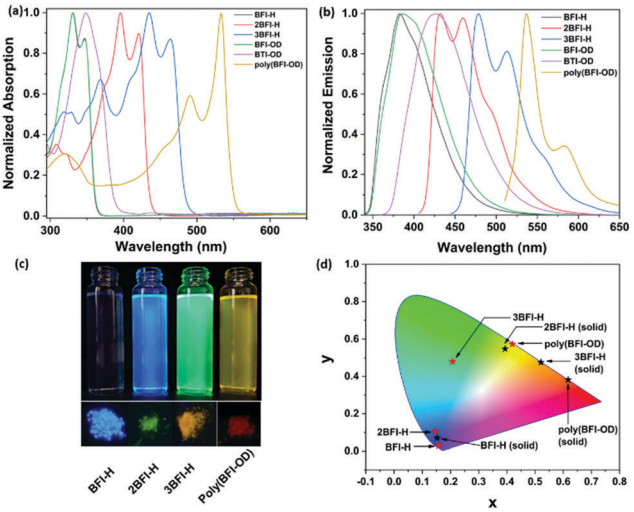

Fig. 3 Normalized (a) UV-Vis absorption and (b) fluorescence spectra of **BFI-H**, **2BFI-H**, **3BFI-H**, **BFI-OD**, **BTI-OD**, and poly(**BFI-OD**) in $CHCl_3$ at room temperature; (c) photograph of fluorescence emission of **BFI-H**, **2BFI-H**, **3BFI-H**, and poly(**BFI-OD**): (top) in $CHCl_3$ solution and (bottom) in the solid state at 365 nm; (d) emission colors of **BFI-H**, **2BFI-H**, **3BFI-H**, and poly(**BFI-OD**) on the CIE 1931 chromaticity diagram.

the thiophene analogue, **BTI-OD**,[32] for comparison. While all the furan-containing analogues display clear vibronic shoulders in the absorption spectra, the featureless appearance of the **BTI-OD** spectrum indicates its more flexible backbone. An additional indication of the greater rigidity of the furan-containing analogues is their lower Stokes shift (0.52 eV *vs.* 0.66 eV for **BFI-OD** and **BTI-OD**, respectively). The dimer and trimer display a smaller Stokes shift of 0.26 eV for both (Table 1). The polymer, poly(**BFI-OD**), also displays similar features, with λ_{abs} = 532 nm and λ_{em} = 537 nm, indicating a rigid backbone, despite the high solubility (Table 1). No significant solvatochromic shift was observed for the absorption spectra upon increasing solvent polarity from hexane to acetonitrile (Fig. S5, S6, S8–S11 and Table S1, ESI†), indicating that the lowest energy transition (π–π^*) has an apolar nature. The optical energy gap ($E_{g(opt)}$) ranges between 3.44 eV for **BFI-H** to 2.26 eV for poly(**BFI-OD**) (Table 1). The solid state (film) absorption and fluorescence spectra experience a bathochromic shift of up to 0.35 eV, and $E_{g(opt)}$ is lower by 0.34–0.1 eV compared with the values in measured chloroform (the film $E_{g(opt)}$ ranges between 3.10 eV for **BFI-H** to 2.16 eV for poly(**BFI-OD**), Fig. S7 and Table S1, ESI†).

Fig. 3c shows the fluorescence images of **BFI-H**, **2BFI-H**, **3BFI-H**, and poly(**BFI-OD**) in solution ($CHCl_3$) and in the solid state at 365 nm. The fluorescence quantum efficiencies (Φ_f) range between 0.65 and 0.81 for all oligomers, and remain high for the polymer poly(**BFI-OD**), with Φ_f = 0.71 (Table 1). Fig. 3d places **BFI-H**, **2BFI-H**, **3BFI-H**, and poly(**BFI-OD**) on the ICE 1931 chromaticity diagram in solution ($CHCl_3$) and in the solid state. **BFI-H** shows relatively high solid-state quantum efficiency with Φ_f = 0.18, despite having strong π–π interactions (Fig. 2a), and the combination of these factors with ICE coordinates of (0.15, 0.07), close to those of the European Broadcasting Union (EBU) blue standard (0.15, 0.06), renders it a good candidate for blue light emitting devices. The fluorescence rate (k_f) and non-radiative decay rate (k_{NR}) do not change dramatically upon backbone elongation, with poly(**BFI-OD**) (k_f = 0.44 and k_{NR} = 0.18 ns^{-1}) and **2BFI-H** (k_f = 0.46 and k_{NR} = 0.11 ns^{-1}) displaying similar values. This is another indication of the backbone rigidity of the polymer (Table 1).

As oligofurans are prone to photooxidation, we examined the ambient photostability of **BFI**-containing materials in comparison with quaterfuran (**4F**) measured under the same conditions. While **4F** undergoes rapid photobleaching, with less than 50% of the initial absorption remaining after 2 h (Fig. 4, and Fig. S12, ESI†), **BFI-H** and **2BFI-H** (having similar λ_{abs} values and extinction coefficients as **4F**) show negligible bleaching, even after prolonged (24 h) exposure. It is important to note that both **2BFI-H** and **4F** have similar λ_{abs} values and extinction coefficients. Longer oligomers show more significant bleaching, but are considerably more stable than **4F**, with less than 10% bleaching after 24 h for poly(**BFI-OD**). Our previous efforts to obtain polyfurans by chemical polymerization always resulted in materials that undergo rapid photobleaching. To the best of our knowledge, poly(**BFI-OD**) is the first chemically prepared polyfuran homopolymer stable under such conditions.

As the HOMO levels of **nF** are higher than those of the corresponding **nT** by approximately 0.35 eV, **nF** are considered

Table 1 Photophysical data of bifuran-imide-based compounds

Compounds	λ_{abs}[a] (nm)	λ_{em}[a] (nm)	Stokes shift (eV)	ε[a] (M^{-1} cm^{-1})	Φ_f[a]	Φ_f (solid)	τ_F[a] (ns)	k_F[b] (ns^{-1})	k_{NR}[c] (ns^{-1})	$E_{g(opt)}$[d] [eV]	HOMO [eV]
BFI-H	330, 343	383	0.52	13 714	0.80	0.18	4.14	0.19	0.05	3.44	−6.05
2BFI-H	396, 415	432, 459	0.26	37 353	0.81	0.06	1.74	0.46	0.11	2.85	−5.71
3BFI-H	365, 435, 457	478, 513	0.26	57 600	0.65	0.06	1.78	0.36	0.20	2.57	−5.69
BFI-OD	331, 344	385	0.52	10 318	0.77	—	4.08	0.19	0.06	3.44	−5.94
BTI-OD	348	427	0.66	11 670	0.78	—	5.83	0.13	0.04	3.22	−6.03
Poly(**BFI-OD**)	492, 532	537, 584	0.02	—	0.71	0.05	1.61	0.44	0.18	2.26	−6.30

[a] Measured in the $CHCl_3$. [b] Calculated according to the equation $k_F = \Phi_f/\tau_F$. [c] Calculated according to the equation $\Phi_f = k_F/(k_F + k_{NR})$. [d] $E_{gap} = 1242/\lambda_{onset}$; $E_{HOMO} = -\left(4.8 - E^{1/2}_{Fc/Fc^+} + E^{ox1}_{onset}\right)$.[39]

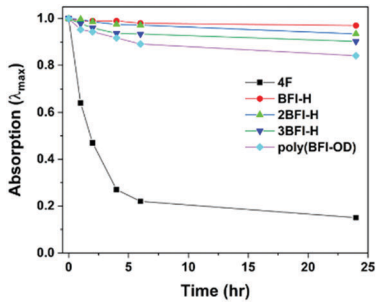

Fig. 4 Photostability of solutions of **4F**, **BFI-H**, **2BFI-H**, **3BFI-H**, and poly(**BFI-OD**) in 1,4-dioxane in ambient light at room temperature.

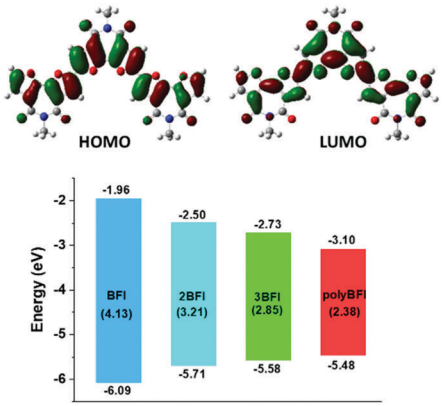

Fig. 5 (top) Frontier molecular orbitals of **3BFI** and (bottom) calculated (B3LYP/6-31G(d)) energy levels of the HOMO (bottom values) and LUMO (top values), and the HOMO–LUMO gaps (middle) of the bifuran-imides discussed (in eV).

p-type materials. However, high HOMO levels greatly contribute to their ambient instability. The calculated (B3LYP/6-31G(d)) HOMO and LUMO levels of **nBFI** are depicted in Fig. 5. Unlike the corresponding **BTI**, which can be considered n-type materials, the HOMO level remains high for **BFI**, with **3BFI** having HOMO and LUMO levels (−5.58 and −2.73 eV respectively) similar to those of sexithiophene (**6T**). The calculated (PBC/B3LYP/6-31G(d)) band gap of poly(**BFI-OD**) is 2.38 eV, similar to that of parent polyfurans calculated at the same level of theory. However absolute energy of the HOCO and LUCO levels of poly(**BFI-OD**), being −5.48 and −3.10 eV respectively, are 0.9 eV lower, which accounts for their high stability (both thermally and photochemically) compared with the corresponding polyfurans. The HOMO levels were also estimated using the oxidation potential measured by cyclic voltammetry (Table 1 and Fig. S34, ESI†), which revealed a good match to the calculated values.

Conclusions

In summary, we have introduced a new building unit, bifuranimide (**BFI**), and its corresponding oligomers and homopolymer, as a new family of π-conjugated backbones. The polymer poly(**BFI-OD**) displayed high solubility and has a higher molecular weight compared with its thiophene analogues. The strong quinoid character of **nBFI** is evident from the short interring bond in their X-ray structures, the vibronic features in their absorption spectra, and their low Stokes shifts. The obtained oligomers and polymers exhibit strong fluorescence with quantum yields reaching up to 81% in solution. The monomer, **BFI-H**, also demonstrates strong blue emission in the solid state. Compared with their parent oligofurans, bifuran-imides are significantly more stable under ambient conditions. Overall, this study establishes **BFI** as a stable furan building unit for organic electronics.

Conflicts of interest

There are no conflicts to declare.

Acknowledgements

The work is supported by the German-Israeli Foundation for Scientific Research and Development. We thank Dr K. S. N. Raju, for his assistance in GPC measurements.

Notes and references

1 H. Huang, L. Yang, A. Facchetti and T. J. Marks, *Chem. Rev.*, 2017, **117**, 10291–10318.
2 H. Usta, A. Facchetti and T. J. Marks, *Acc. Chem. Res.*, 2011, **44**, 501–510.
3 A. Pron, P. Gawrys, M. Zagorska, D. Djurado and R. Demadrille, *Chem. Soc. Rev.*, 2010, **39**, 2577–2632.
4 M. Irimia-Vladu, *Chem. Soc. Rev.*, 2014, **43**, 588–610.
5 M. E. Cinar and T. Ozturk, *Chem. Rev.*, 2015, **115**, 3036–3140.
6 A. Mishra, C.-Q. Ma and P. Bäuerle, *Chem. Rev.*, 2009, **109**, 1141–1276.
7 M. Iyoda and H. Shimizu, *Chem. Soc. Rev.*, 2015, **44**, 6411–6424.
8 L. Zhang, N. S. Colella, B. P. Cherniawski, S. C. B. Mannsfeld and A. L. Briseno, *ACS Appl. Mater. Interfaces*, 2014, **6**, 5327–5343.
9 *Handbook of Thiophene-Based Materials*, ed. I. F. Perepichka and D. F. Perepichka, John Wiley & Sons, Ltd., 2009.
10 Y. Shi, H. Guo, M. Qin, J. Zhao, Y. Wang, H. Wang, Y. Wang, A. Facchetti, X. Lu and X. Guo, *Adv. Mater.*, 2018, **30**, 1705745.
11 O. Gidron, Y. Diskin-Posner and M. Bendikov, *J. Am. Chem. Soc.*, 2010, **132**, 2148–2150.
12 O. Gidron, A. Dadvand, Y. Sheynin, M. Bendikov and D. F. Perepichka, *Chem. Commun.*, 2011, **47**, 1976–1978.
13 O. Gidron, A. Dadvand, E. W.-H. Sun, I. Chung, L. J. W. Shimon, M. Bendikov and D. F. Perepichka, *J. Mater. Chem. C*, 2013, **1**, 4358–4367.
14 O. Gidron, N. Varsano, L. J. W. Shimon, G. Leitus and M. Bendikov, *Chem. Commun.*, 2013, **49**, 6256–6258.
15 X.-H. Jin, D. Sheberla, L. J. W. Shimon and M. Bendikov, *J. Am. Chem. Soc.*, 2014, **136**, 2592–2601.
16 O. Dishi and O. Gidron, *J. Org. Chem.*, 2018, **83**, 3119–3125.
17 H. Cao and P. A. Rupar, *Chem. – Eur. J.*, 2017, **23**, 14670–14675.

 This journal is © The Royal Society of Chemistry 2018

18 J. Mei, H. C. Wu, Y. Diao, A. Appleton, H. Wang, Y. Zhou, W. Y. Lee, T. Kurosawa, W. C. Chen and Z. Bao, *Adv. Funct. Mater.*, 2015, **25**, 3455–3462.

19 S. Zhen, B. Lu, J. Xu, S. Zhang and Y. Li, *RSC Adv.*, 2014, **4**, 14001–14012.

20 Y. Qiu, A. Fortney, C.-H. Tsai, M. A. Baker, R. R. Gil, T. Kowalewski and K. J. T. Noonan, *ACS Macro Lett.*, 2016, **5**, 332–336.

21 M. Jeffries-El, B. M. Kobilka and B. J. Hale, *Macromolecules*, 2014, **47**, 7253–7271.

22 O. Gidron and M. Bendikov, *Angew. Chem., Int. Ed.*, 2014, **53**, 2546–2555.

23 S. Sharma and M. Bendikov, *Chem. – Eur. J.*, 2013, **19**, 13127–13139.

24 I. F. Perepichka, D. F. Perepichka, H. Meng and F. Wudl, *Adv. Mater.*, 2005, **17**, 2281–2305.

25 S. Reineke, F. Lindner, G. Schwartz, N. Seidler, K. Walzer, B. Lüssem and K. Leo, *Nature*, 2009, **459**, 234.

26 I. F. Perepichka, D. F. Perepichka and H. Meng, in *Handbook of Thiophene-Based Materials*, ed. I. F. Perepichka and D. F. Perepichka, John Wiley & Sons, Ltd., 2009, p. 695.

27 P. Sonar, T. R. B. Foong, S. P. Singh, Y. Li and A. Dodabalapur, *Chem. Commun.*, 2012, **48**, 8383–8385.

28 P. Sonar, S. P. Singh, E. L. Williams, Y. Li, M. S. Soh and A. Dodabalapur, *J. Mater. Chem.*, 2012, **22**, 4425–4435.

29 J. C. Bijleveld, B. P. Karsten, S. G. J. Mathijssen, M. M. Wienk, D. M. de Leeuw and R. A. J. Janssen, *J. Mater. Chem.*, 2011, **21**, 1600–1606.

30 Y. Li, P. Sonar, S. P. Singh, W. Zeng and M. S. Soh, *J. Mater. Chem.*, 2011, **21**, 10829–10835.

31 S. Gadakh, L. J. W. Shimon and O. Gidron, *Angew. Chem., Int. Ed.*, 2017, **44**, 13601–13605.

32 J. A. Letizia, M. R. Salata, C. M. Tribout, A. Facchetti, M. A. Ratner and T. J. Marks, *J. Am. Chem. Soc.*, 2008, **130**, 9679–9694.

33 X. Guo, R. P. Ortiz, Y. Zheng, Y. Hu, Y.-Y. Noh, K.-J. Baeg, A. Facchetti and T. J. Marks, *J. Am. Chem. Soc.*, 2011, **133**, 1405–1418.

34 M. Saito, I. Osaka, Y. Suda, H. Yoshida and K. Takimiya, *Adv. Mater.*, 2016, **28**, 6921–6925.

35 Y. Wang, Z. Yan, H. Guo, M. A. Uddin, S. Ling, X. Zhou, H. Su, J. Dai, H. Y. Woo and X. Guo, *Angew. Chem., Int. Ed.*, 2017, **56**, 15304–15308.

36 Y. Wang, H. Guo, S. Ling, I. Arrechea-Marcos, Y. Wang, J. T. L. Navarrete, R. P. Ortiz and X. Guo, *Angew. Chem., Int. Ed.*, 2017, **56**, 9924–9929.

37 Y. Wang, H. Guo, A. Harbuzaru, M. A. Uddin, I. Arrechea-Marcos, S. Ling, J. Yu, Y. Tang, H. Sun, J. T. López Navarrete, R. P. Ortiz, H. Y. Woo and X. Guo, *J. Am. Chem. Soc.*, 2018, **140**, 6095–6108.

38 H. Cao, I. A. Brettell-Adams, F. Qu and P. A. Rupar, *Organometallics*, 2017, **36**, 2565–2572.

39 N. G. Connelly and W. E. Geiger, *Chem. Rev.*, 1996, **96**, 877–910.